J|A|C|S
ARTICLES
Published on Web 01/23/2003

Heterogeneous Electron-Transfer Kinetics for Ruthenium and Ferrocene Redox Moieties through Alkanethiol Monolayers on Gold

John F. Smalley,*,† Harry O. Finklea,‡ Christopher E. D. Chidsey,§ Matthew R. Linford,|| Stephen E. Creager,⊥ John P. Ferraris,▽ Keli Chalfant,† Thomas Zawodzinsk,○ Stephen W. Feldberg,† and Marshall D. Newton#

Contribution from the Materials Science Department and Chemistry Department, Brookhaven National Laboratory, Upton, New York 11973-5000, Department of Chemistry, West Virginia University, Morgantown, West Virginia 26506, Department of Chemistry, Stanford University, Stanford, California 94305-5080, Department of Chemistry & Biochemistry, Brigham Young University, Provo, Utah 84602, Department of Chemistry, Clemson University, Clemson, South Carolina 29634, Department of Chemistry, University of Texas at Dallas, Richardson, Texas 75083, and Department of Chemical Engineering, Case Western Reserve University, Cleveland, Ohio 44106-7217

Received September 7, 2002; E-mail: smalley@bnl.gov

Abstract: The standard heterogeneous electron-transfer rate constants between substrate gold electrodes and either ferrocene or pentaaminepyridine ruthenium redox couples attached to the electrode surface by various lengths of an alkanethiol bridge as a constituent of a mixed self-assembled monolayer were measured as a function of temperature. The ferrocene was either directly attached to the alkanethiol bridge or attached through an ester (CO_2) linkage. For long bridge lengths (containing more than 11 methylene groups) the rate constants were measured using either chronoamperometry or cyclic voltammetry; for the shorter bridges, the indirect laser induced temperature jump technique was employed to measure the rate constants. Analysis of the distance (bridge length) dependence of the preexponential factors obtained from an Arrhenius analysis of the rate constant versus temperature data demonstrates a clear limiting behavior at a surprisingly small value of this preexponential factor (much lower than would be expected on the basis of aqueous solvent dynamics). This limit is independent of both the identity of the redox couple and the nature of the linkage of the couple to the bridge, and it is definitely different (smaller) from the limit derived from an equivalent analysis of the rate constant (versus temperature) data for the interfacial electron-transfer reaction through oligophenylenevinylene bridges between gold electrodes and ferrocene. There are a number of possible explanations for this behavior including, for example, the possible effects of bridge conformational flexibility upon the electron-transfer kinetics. Nevertheless, conventional ideas regarding electronic coupling through alkane bridges and solvent dynamics are insufficient to explain the results reported here.

Introduction

There is a continuing interest in the study of the kinetics of electron transfer of redox moieties irreversibly attached to metal surfaces (electrodes) as a part of a stable, organized structure.[1−3] There are many reasons for this interest: a significant amount of the redox moiety is located at a well-defined distance from the electrode, that distance can be varied as can the chemical composition of the bridge, diffusive and convective transport are eliminated as complicating factors, and adsorption, which can seriously complicate studies of solution-based systems, is also eliminated. Consequently, these systems are ideal for the experimental study of the fundamental physical and chemical factors (other than transport) which control the rate of interfacial electron-transfer and homogeneous electron-transfer reactions[4−9] and long-range electron transfer in biological structures.[9−11]

† Materials Science Department, Brookhaven National Laboratory.
‡ West Virginia University.
§ Stanford University.
|| Brigham Young University.
⊥ Clemson University.
▽ University of Texas at Dallas.
○ Case Western Reserve University.
Chemistry Department, Brookhaven National Laboratory.

(1) Finklea, H. O. In *Electroanalytical Chemistry*; Bard, A. J., Rubinstein, I., Eds.; Marcel Dekker: New York, 1996; Vol. 19, pp 109−335.
(2) Newton, M. D.; Feldberg, S. W.; Smalley, J. F. In *Interfacial Electrochemistry, Theory, Experiment, and Applications*; Wieckowski, A., Ed.; Marcel Dekker: New York, 1999; pp 97−114.
(3) Sachs, S. B., Ph.D. Thesis, Stanford University, Stanford, CA, 2000.
(4) For example, see: (a) Xu, J.; Li, H.-L.; Zhang, Y. *J. Phys. Chem.* **1993**, *97*, 11497. (b) Forster, R. J.; Faulkner, L. R. *J. Am. Chem. Soc.* **1994**, *116*, 5453. (c) Forster, R. J.; Loughman, P.; Keyes, T. E. *J. Am. Chem. Soc.* **2000**, *122*, 11948.
(5) Miller, C. J. In *Physical Electrochemistry, Principles, Methods and Applications*; Rubinstein, I., Ed.; Marcel Dekker: New York, 1995; pp 27−79.
(6) Paddon-Row, M. N. *Acc. Chem. Res.* **1994**, *27*, 18.
(7) Fox, M. A. *Acc. Chem. Res.* **1999**, *32*, 201.
(8) Closs, G. L.; Miller, J. R. *Science* **1988**, *240*, 440.
(9) Wasielewski, M. R. *Chem. Rev.* **1992**, *92*, 435.

 10.1021/ja028458j CCC: $25.00

Studies of attached redox systems may also impact the rapidly developing field of molecular electronics.[12,13]

The electronic coupling (and, consequently, the rate of nonadiabatic interfacial electron transfer) between an attached redox moiety and an electrode is strongly dependent upon the nature and chemical bonding within the bridge.[14] A variety of bridges have, therefore, been investigated. Li and Weaver determined the rate of irreversible reduction of cobalt(III) complexes attached to gold electrodes by thioalkylcarboxylate ligands.[15] However, the interface in the Li and Weaver system lacked a well-defined (and characterized) structure, and the compounds investigated in this study did not constitute a homologous series. To properly characterize the electron-transfer kinetics of attached redox couples, these systems should be a part of a well-defined and organized structure such as those which exist in self-assembled monolayers (SAMs) and the bridges should be in a homologous series.[16,17] In such mixed self-assembled monolayer systems (consisting of the tethered redox moiety and a diluent species both covalently attached to the surface of the electrode) the dependence of the rate constants (k_{et}) on the molecular length of the bridge (l) for putatively single-step, long-distance electron-transfer reactions may be conveniently studied and the exponential decay constants ($\beta = -(\mathrm{d} \ln [k_{et}])/\mathrm{d}l$) for the distance dependencies of these reactions determined. A number of studies from our laboratories (investigating both ferrocene[16−22] and pentaaminepyridine ruthenium[23−28] redox couples attached to the bridge through a variety of functional groups) have determined that $\beta \approx 1.0$ Å^{-1} for electron transfer through saturated alkane bridges which were part of SAMs. For self-assembled monolayers containing ferrocene attached to gold electrodes through unsaturated oligophenyleneethynylene (OPE) bridge, we have reported β values ranging from ∼0.4 to ∼0.6 Å^{-1}.[11,14,29]

Because the low barrier to rotation of the phenylene rings in the OPE bridge may result in incomplete conjugation of these bridges, interfacial electron transfer of ferrocene through the much more rigid oligophenylenevinylene (OPV) bridges has recently been investigated.[31] The electron-transfer rate constants observed with these OPV bridges are larger than those observed with other bridges of comparable length, and the distance dependence of the OPV Arrhenius prefactors (A_n in eq 1, where E_A is the corresponding Arrhenius activation energy and $k°$ is the standard rate constant for the electron-transfer reaction) is exceedingly low ($-(\mathrm{d} \ln [A_n])/\mathrm{d}l \approx 0.06$ Å^{-1}).

$$k° = A_n \exp[-E_A/RT] \quad (1)$$

The unusually small distance dependence observed for the OPV Arrhenius prefactors indicates that the rate of electron transfer is not determined by the size of the electronic coupling between the ferrocene redox moiety and the gold electrode.[31] Furthermore, the magnitudes of these prefactors are at least an order of magnitude lower than the rate expected for aqueous solvent dynamics (at 25 °C). This suggests that some other process limits the rate. Because this process may involve the bridge, it would be of interest to investigate other bridges to see if (and where) the Arrhenius prefactors limit.

Some of us have already observed an indication that the Arrhenius prefactors for the electron transfer of ferrocene attached to an alkanethiol bridge through an ester group limit at short alkane chain lengths.[17] Accordingly, we have employed the unique capabilities of the indirect laser induced temperature jump (ILIT) technique[17,32−35] to measure, as a function of temperature and the length of the bridge, the electron-transfer rate constants of ferrocene directly attached to alkanethiol bridges and pentaaminepyridine ruthenium redox centers whose alkanethiol bridges contain an amide ($-CONHCH_2^-$) linkage. In the present study, rate data were measured for these redox couple/bridge combinations at shorter bridge lengths than studied previously, and most importantly, the rate data at all bridge lengths studied here have not been previously[21,28] determined over a range of temperatures. Both the oxidized and reduced forms of the ruthenium redox center are charged (+3 and +2, respectively) so that hydrophobic interactions with the film might be expected to be smaller than with the ferrocene couple. Additionally, because the ILIT response is a change in the open circuit potential, uncompensated solution resistance has no effect on measured standard rate constants.

Arrhenius prefactors were determined for the redox couple/bridge combinations studied here from the temperature dependencies of the respective $k°$. When these prefactors are combined with those measured for ferrocene attached to the alkanethiol bridge through an ester linkage at both short and long bridge lengths, a clear limiting behavior is observed with the limit being independent of both the identity of the redox couple and the nature of the linkage to the alkane portion of the bridge, suggesting that factors other than electronic coupling or solvent dynamics may be rate limiting and that these rate-limiting phenomena are associated with the bridge. The suggestion that the reactions studied here are "gated" processes[36−38] will be

(10) Winkler, J. R.; Gray, H. B. *Chem. Rev.* **1992**, *92*, 369.
(11) Creager, S.; Yu, C. J.; Bamdad, C.; O'Connor, S., MacLean, T.; Lam, E.; Chang, Y.; Olsen, G. T.; Luo, J.; Gozin, M.; Kayyem, J. F. *J. Am. Chem. Soc.* **1999**, *121*, 1059.
(12) Mirkin, C. A.; Ratner, M. A. *Annu. Rev. Phys. Chem.* **1992**, *92*, 369.
(13) Joachim, C.; Ginzewski, J. K.; Aviram, A. *Nature* **2000**, *408*, 541.
(14) Sachs, S. B.; Dudek, S. P.; Hsung, R. P.; Sita, L. R.; Smalley, J. F.; Newton, M. D.; Feldberg, S. W.; Chidsey, C. E. D. *J. Am. Chem. Soc.* **1997**, *119*, 10563.
(15) Li, T. T.-T.; Weaver, M. J. *J. Am. Chem. Soc.* **1984**, *106*, 6107.
(16) Chidsey, C. E. D. *Science* **1991**, *251*, 919.
(17) Smalley, J. F.; Feldberg, S. W.; Chidsey, C. E. D.; Linford, M. R.; Newton, M. D.; Liu, Y.-P. *J. Phys. Chem.* **1995**, *99*, 13141.
(18) Weber, K.; Creager, S. E. *Anal. Chem.* **1994**, *66*, 3164.
(19) Richardson, J. N.; Peck, S. R.; Curtin, L. S.; Tender, L. M.; Terrill, R. H.; Carter, M. T.; Murray, R. W.; Rowe, G. K.; Creager, S. E. *J. Phys. Chem.* **1995**, *99*, 766.
(20) Weber, K.; Hockett, L.; Creager, S. E. *J. Phys. Chem. B* **1997**, *101*, 8286.
(21) Sumner, J. J.; Weber, K. S.; Hockett, L. A.; Creager, S. E. *J. Phys. Chem. B* **2000**, *104*, 7449.
(22) Sumner, J. J.; Creager, S. E. *J. Am. Chem. Soc.* **2000**, *122*, 11914.
(23) Finklea, H. O.; Hanshew, D. D. *J. Am. Chem. Soc.* **1992**, *114*, 3173.
(24) Finklea, H. O.; Ravenscroft, M. S.; Snider, D. A. *Langmuir* **1993**, *9*, 223.
(25) Ravenscroft, M. S., Finklea, H. O. *J. Phys. Chem.* **1994**, *98*, 3843.
(26) Finklea, H. O.; Liu, L.; Ravenscroft, M. S.; Punturi, S. *J. Phys. Chem.* **1996**, *100*, 18852.
(27) Finklea, H. O.; Ravenscroft, M. S. *Isr. J. Chem.* **1997**, *37*, 179.
(28) Brevnov, D. A.; Finklea, H. O.; Van Ryswyk, H. *J. Electroanal. Chem.* **2001**, *500*, 100.
(29) However, some of us[30] have recently observed that the distance dependence of the ferrocene (redox couple)/unsubstituted OPE (bridge) electron-transfer rate constants is not monotonic.
(30) Sachs, S. B.; Dudek, S. P.; Sikes, H. D.; Chidsey, C. E. D.; Feldberg, S. W.; Newton, M. D.; Smalley, J. F. Unpublished data.
(31) Sikes. H. D.; Smalley, J. F.; Dudek, S. P.; Cook, A. R.; Newton, M. D.; Chidsey, C. E. D.; Feldberg, S. W. *Science* **2001**, *291*, 1519.
(32) Smalley, J. F.; Krishnan, C. V.; Goldman, M.; Feldberg, S. W.; Ruzic, I. *J. Electroanal. Chem.* **1988**, *248*, 255.
(33) Smalley, J. F.; MacFarquhar, R. A.; Feldberg, S. W. *J. Electroanal. Chem.* **1988**, *256*, 21.
(34) Smalley, J. F.; Geng, L.; Feldberg, S. W.; Rogers, L. C.; Leddy, J. *J. Electroanal. Chem.* **1993**, *356*, 181.
(35) Smalley, J, F.; Newton, M. D.; Feldberg, S. W. *Electrochem. Commun.* **2000**, *2*, 832.
(36) Hoffman, B. M.; Ratner, M. A. *J. Am. Chem. Soc.* **1987**, *109*, 6237.

introduced, and possible technological implications for the results reported here will also be discussed.

Experimental Section

The ILIT Technique. The ILIT apparatus, cell, electrodes, and experimental techniques have all been described in detail elsewhere.[17,32,34] Briefly, in the ILIT technique, a short (~10 ns in the present apparatus) laser pulse impinges onto the backside of a thin (~1 μm in this work) gold film electrode which has been vapor deposited over a 500 Å thick layer of titanium vapor deposited on a quartz disk. The microcrystallites comprising the gold electrode surface have a uniform 111 orientation.[17] The absorbed laser energy is rapidly (within ~1 ps) degraded into heat which quickly (within ~4 ns) diffuses through the gold film and causes a small change (2−4 °C) in the temperature of the electrode/electrolyte solution interface at the front side of the gold film. This change in temperature disturbs the interfacial equilibrium and effects a change in the open circuit potential of the electrode, which is the quantity measured. In the presence of a redox couple, the time dependence of this change in the open circuit potential is a function of the decay of the thermal perturbation and the rate of electron transfer between the electrode and the redox moieties.

The open circuit potential (ILIT) transients were fit to[17,34]

$$\Delta V(t) = A'\Delta T^*(t) + B'k_m(E_i)\int_0^t e^{-k_m(t-\tau)}\,\Delta T^*(\tau)\,d\tau \qquad (2)$$

where $\Delta V(t)$ is the change in the open circuit potential as a function of time, A' is the amplitude of the (initial) thermal response, B' is the amplitude of the electron-transfer relaxation, and $k_m(E_i)$ (= k_m) is the measured (experimental) rate constant (s^{-1}) for this relaxation at the initial (applied) potential (E_i). $\Delta T^*(\tau)$ in eq 2 is the convolution of the temperature perturbation at the electrode/electrolyte interface and the instrument response function divided by the interfacial temperature change (ΔT_{eq}) that would be produced if all of the absorbed heat were uniformly distributed in the electrode and none of this heat were lost to either the quartz disk or the electrolyte solution.[17,34] Standard electron-transfer rate constants ($k°$, the rate constant at the formal potential ($E°'$) of the redox couple) were obtained from fits of plots of k_m versus E_i to[35]

$$k_m(E_i) = k°\frac{\gamma\omega(E_i)^{1/2}}{1+\omega(E_i)}\left\{1 + \frac{[1+\omega(E_i)]^2}{\gamma\omega(E_i)}\right\} \qquad (3)$$

where

$$\gamma = N_T F^2/RTC_{film} \qquad (4)$$

and

$$\omega(E_i) = \exp[(F/RT)(E_i - E°')] \qquad (5)$$

In eqs 4 and 5, F is the Faraday constant, R is the ideal gas constant, T is the absolute temperature, N_T is the number of redox species attached to the electrode (mol), and C_{film} is the double-layer capacitance of the electrode/electrolyte interface (F). Values of γ and $E°'$ may be derived from either the fit of k_m vs E_i to eqs 3 and 5 or the cyclic voltammogram (CV) for a SAM containing one of the attached redox couples.

Materials and Methods. The syntheses of the directly linked ferrocenyl-*n*-alkanethiols ($Fc(CH_2)_nSH$, where n = 5, 6, 8, 9, 11, and 16) are described elsewhere.[21,39] For the ILIT experiments, mixed self-assembled monolayers containing these compounds were prepared by placing a cleaned gold film electrode into an ethanol solution containing the redox-active thiol and an alkanethiol diluent molecule of the appropriate length ($HS(CH_2)_mCH_3$, where $m = n - 1$). The total concentration of thiol in these coating solutions was approximately 1.0×10^{-3} M, and the mole fraction of the redox-active thiol was varied to give different concentrations of the redox couple in the monolayer. The electrodes remained in these coating solutions for approximately 16 h (overnight), were rinsed in neat ethanol (or ethanol and hexane), were dried in a stream of argon, and were attached to the ILIT cell containing the 1.0 or 0.10 M $HClO_4$ aqueous electrolyte solution.

Procedures for the syntheses of the 8-mercaptoctanoic acid, the 6-mercaptohexanoic acid, the dibutanoic acid disulfide,[40] and the [(4-aminomethylpyridine)$Ru(NH_3)_5]^{2+}$ (Ru(4-AMP)) are all described elsewhere.[28,41,44] For the ruthenium redox couple, mixed self-assembled monolayers were prepared by placing a cleaned gold film electrode into a 1.0×10^{-3} M solution of the mercaptocarboxylic acid (or the dibutanoic disulfide) in ethanol. The electrode remained in this first coating solution for between 16 and 36 h. After deposition of the carboxylic acid terminated monolayer, the electrode was removed from this coating solution, rinsed in a succession of ethanol and water, and placed in 10 mL of a second coating solution containing 0.15 g of KNO_3, 0.15 g of EDC (1-[3-(dimethylamino)propyl]-3-ethylcarbodiimide hydrochloride), and between 7×10^{-3} and 9×10^{-3} g of Ru(4-AMP). This second coating solution contained 5×10^{-3} M Na_2HPO_4 adjusted to a pH between 7.0 and 8.0 with H_3PO_4 and was deoxygenated with argon before use. The electrode remained in the second coating solution for between 6 and 15 min, forming amide links between the Ru(4-AMP) and the pendant −COOH functional groups. The electrode was then removed from the second coating solution, rinsed in a succession of water and ethanol, and placed back into the first coating solution for between 6 and 10 min. After this time in the first coating solution, the electrode was rinsed in ethanol, dried in a stream of argon, and attached to the ILIT cell as before. For this redox couple, the electrolyte solution was 0.5 M NaF (pH adjusted to ca. 4.8 with 1.0 M $HClO_4$).

In this paper we also report chronoamperometric measurements of the electron rate constants (as a function of temperature) of long-chained, ester-linked ferrocenyl-*n*-alkanethiols ($HS(CH_2)_nOC(O)Fc$, where n = 12 and 18). The experimental methods used in these measurements are fully described in refs 16 and 45, and the synthesis of these ester-linked ferrocene-terminated alkanethiols is described in ref 45. For the cyclic voltammetry experiment on monolayers containing $Fc(CH_2)_{16}SH$, the methods are described in ref 18.

Aldrich alkanethiols, Baker Ultrex ultrapure $HClO_4$, Aldrich 99.99% pure NaF, Mallinckrodt reagent grade KNO_3, Aaper absolute ethyl alcohol, and Baker reagent grade Na_2HPO_4 and H_3PO_4 were all used as received. The gold film electrodes used in this work were cleaned in an argon ion plasma before use. Cyclic voltammograms of the SAMs investigated in this work were taken before each ILIT experiment on a BAS 100BW electrochemical analyzer, and a saturated sodium calomel reference electrode (SSCE) was used in all experiments. Water was purified in a Millipore Mill-Q Plus system.

Relevant Electron-Transfer Theory. An important aspect of our study is the temperature dependence of the standard electron-transfer rate constant, $k°$. As we have done previously,[31] to accomplish a simple and consistent analysis of the temperature dependence of $k°$ over the entire range of l (bridge length) investigated,[4c] these data were fit to eq 1. If the electronic coupling (H_{ab}) between the redox moiety and

(37) Brunschwig, B. S.; Sutin, N. *J. Am. Chem. Soc.* **1989**, *111*, 7454.
(38) Hoffman, B. M.; Ratner, M. A.; Wallin, S. A. *Adv. Chem. Ser.* **1990**, *226*, 125.
(39) Creager, S. E.; Rowe, G. K. *J. Electroanal. Chem.* **1994**, *370*, 203.
(40) The formation and the exchange kinetics of the adsorbed species[41−43] as well as the position of the X-ray photoelectron spectroscopy 2p peak of the adsorbed sulfur[41] demonstrate that both thiols and disulfides react with gold surfaces to form the same species.
(41) Bain, C. D.; Troughton, E. B.; Tao, Y.-T.; Evall, J.; Whitesides, G. M.; Nuzzo, R. G. *J. Am. Chem. Soc.* **1989**, *111*, 321. See the Supporting Information accompanying this reference for the synthetic procedure.
(42) Biebuyck, H. A.; Whitesides, G. M. *Langmuir* **1993**, *9*, 1766.
(43) Biebuyck, H. A.; Bain, C. D.; Whitesides, G. M. *Langmuir* **1994**, *10*, 1825.
(44) Finklea, H. O.; Hanshew, D. D. *J. Electroanal. Chem.* **1993**, *347*, 327.
(45) Chidsey, C. E. D.; Bertozzi, C. R.; Putzinski, T. M.; Mujsce, A. M. *J. Am. Chem. Soc.* **1990**, *112*, 4301.

Table 1. Standard Electron-Transfer Rate Constants (k^o) at $T = 25$ °C, Activation Energies (E_A), Reorganization Energies (λ_{app}),[54] and Arrhenius Preexponential Factors (A_n) Measured Using ILIT for Mixed Monolayers Containing Either the Ferrocene or Ruthenium Redox Couple

couple[a]	n[b]	l^c/Å	diluent	E^o/mV vs SSCE	k^o/s^{-1}	$E_A{}^d$/eV	$\lambda_{app}{}^e$/eV	ln[A_n/s^{-1}]
Fc	5	6.5	$HS(CH_2)_4CH_3$	192	$(1.6 \pm 0.1) \times 10^7$	0.16 ± 0.01	0.66 ± 0.03	22.96 ± 0.77
Fc	6	7.8	$HS(CH_2)_5CH_3$	154	$(2.4 \pm 0.1) \times 10^6$	0.20 ± 0.01	0.78 ± 0.04	22.30 ± 0.79
Fc	8	10.3	$HS(CH_2)_7CH_3$	154	$(4.4 \pm 0.2) \times 10^5$	0.25 ± 0.01	1.00 ± 0.04	22.69 ± 0.78
Fc	9	11.6	$HS(CH_2)_8CH_3$	215	$(1.3 \pm 0.1) \times 10^5$	0.24 ± 0.01	0.97 ± 0.02	21.19 ± 0.64
Fc	11	14.1	$HS(CH_2)_{10}CH_3$	186	$(1.2 \pm 0.1) \times 10^4$	0.24 ± 0.01	0.97 ± 0.05	18.81 ± 0.84
Ru	3	7.6	$[S(CH_2)_3CO_2H]_2$	23	$(5.4 \pm 0.3) \times 10^6$	0.18 ± 0.01	0.74 ± 0.04	22.65 ± 0.82
Ru	5	10.1	$HS(CH_2)_5CO_2H$	22	$(8.9 \pm 0.4) \times 10^5$	0.21 ± 0.01	0.84 ± 0.02	21.82 ± 0.65
Ru	7	12.6	$HS(CH_2)_7CO_2H$	45	$(4.3 \pm 0.2) \times 10^5$	0.21 ± 0.01	0.82 ± 0.04	20.99 ± 0.79
Ru	10	16.4	$HS(CH_2)_{10}CO_2H$	40	$(3.5 \pm 0.2) \times 10^3$	0.22 ± 0.01	0.88 ± 0.02	16.70 ± 0.62

[a] Fc refers to the directly linked ferrocene couple, and Ru refers to (pyridine)$Ru(NH_3)_5$. [b] Number of methylene groups in the alkanethiol constituent of the bridge (note that for Ru the linkage contains an extra CH_2 group). [c] The bridge length (l) for the directly linked (DL) or ester-linked (EL) ferrocene is the shortest distance between the carbon attached to the sulfur and the linked carbon of the cyclopentadiene ring ($l = 0$ when the cyclopentadiene carbon is attached to the sulfur); the bridge length (l) for the ruthenium couples is between the carbon attached to the sulfur and the C4 carbon of the pyridine ($l = 0$ when the C4 is attached to the sulfur). The alkane chains are assumed to be all-trans. [d] Arrhenius activation energy (see the text). [e] Reorganization energy obtained from the Arrhenius analysis[54] (see the text).

Table 2. Activation Energies (E_A), Reorganization Energies (λ_{app}),[54] and Arrhenius Preexponential Factors (A_n) Measured Using Either Chronoamperometry (CA) or Cyclic Voltammetry (CV) for Mixed Monolayers Containing Either the Ester-Linked or Directly Linked Ferrocene Redox Couple

linkage[a]	n[b]	l^c/Å	diluent	technique	$E_A{}^d$/eV	$\lambda_{app}{}^e$/eV	ln[A_n/s^{-1}]
EL	12	17.7	$HS(CH_2)_{11}CH_3$	CA	0.24 ± 0.01	0.96 ± 0.04	13.91 ± 0.88
EL	18	25.2	$HS(CH_2)_{17}CH_3$	CA	0.23 ± 0.01	0.95 ± 0.06	7.20 ± 0.80
DL	16	20.4	$HS(CH_2)_{15}CH_3$	CV	0.24 ± 0.02	0.95 ± 0.09	12.70 ± 0.90

[a] EL refers to the ester-linked and DL refers to the directly linked ferrocene redox couple. [b] Number of methylene groups in the alkanethiol constituent of the bridge. [c] See footnote *c* in Table 1. [d] Arrhenius activation energy (see the text). [e] Reorganization energy obtained from the Arrhenius analysis[54] (see the text).

the electrode is weak (i.e., the interfacial electron-transfer reaction is nonadiabatic), the Arrhenius preexponential factor and activation energy are well approximated by[17,47]

$$A_{n,\mathrm{NA}} = 2\pi^{3/2} H_{\mathrm{ab}}{}^2 \rho_{\mathrm{m}}/h \tag{6}$$

and

$$E_{\mathrm{A,NA}} = \lambda/4 \tag{7}$$

where the subscript "NA" specifically identifies these quantities for a nonadiabatic reaction, ρ_m is the density of electronic states in the metal electrode, h is Planck's contant, and λ is the reorganization energy for the electron-transfer reaction. In principle λ is a free energy and, therefore, is a sum of enthalpic and entropic terms. However, we will present data supporting the argument that, in the present study, the entropic component of λ is always negligibly small so that the activation energy of a purely nonadiabatic reaction (if $H_{ab} \ll \lambda$, see eq 10 below) is always given by eq 7.

Because of image charge effects, the value of λ decreases with decreasing distance between the electrode and the redox moiety as predicted by Marcus[47] for systems involving a metal electrode and solvent. Liu and Newton[48] extended Marcus' treatment to include systems involving a metal electrode, a film (e.g., a SAM), and solvent. The relevant expression is

$$\lambda = \left(\frac{1}{\epsilon_{\mathrm{I}}^{\mathrm{op}}} - \frac{1}{\epsilon_{\mathrm{I}}^{\mathrm{s}}}\right)\frac{(\Delta e)^2}{2a} - \left(\frac{\theta_{\mathrm{II,I}}^{\mathrm{op}}}{\epsilon_{\mathrm{II}}^{\mathrm{op}}} - \frac{\theta_{\mathrm{II,I}}^{\mathrm{s}}}{\epsilon_{\mathrm{I}}^{\mathrm{s}}}\right)\frac{(\Delta e)^2}{4d} + \sum_{n=1}^{\infty}\left(\frac{\epsilon_{\mathrm{II}}^{\mathrm{op}}(\theta_{\mathrm{II,I}}^{\mathrm{op}})^{n-1}(\theta_{\mathrm{II,III}}^{\mathrm{op}})^n}{(\epsilon_{\mathrm{II}}^{\mathrm{op}} - \epsilon_{\mathrm{I}}^{\mathrm{op}})^2} - \frac{\epsilon_{\mathrm{II}}^{\mathrm{s}}(\theta_{\mathrm{II,I}}^{\mathrm{s}})^{n-1}(\theta_{\mathrm{II,III}}^{\mathrm{s}})^n}{(\epsilon_{\mathrm{II}}^{\mathrm{s}} - \epsilon_{\mathrm{I}}^{\mathrm{s}})^2}\right)\frac{(\Delta e)^2}{d + nL} \tag{8}$$

where

$$\theta_{i,j} = \frac{\epsilon_i - \epsilon_j}{\epsilon_i + \epsilon_j} \tag{9}$$

and where subscripts I, II, and III denote the aqueous solution, the film, and the electrode, respectively, L is the thickness of the film, d is the distance of the redox moiety (assumed to be in the solution) from the film/solution interface, a is the cavity radius (=d in our calculations), Δe is the change in charge associated with the redox reaction (1 electronic charge for our systems), and superscripts "op" and "s" denote optical and static values of the dielectric constant, ϵ. (For the aliphatics we assume that $L = 2.1$ Å$+ l \cos(30°)$, where l is the distance specified in Tables 1 and 2.) Additionally, as the coupling strength increases, E_A is lowered and the relationship between E_A and λ becomes more complicated, i.e.[49,50]

$$E_{\mathrm{A}} = \frac{\lambda}{4} - H_{\mathrm{ab}} + \frac{H_{\mathrm{ab}}{}^2}{\lambda} \tag{10}$$

Results and Discussion

Figure 1 shows cyclic voltammograms for both the directly linked ferrocene ($n = 11$; see Table 1) and ruthenium ((pyridine)$Ru(NH_3)_5{}^{3+/2+}$, $n = 10$; see Table 1) redox couples each attached to a Au electrode. The cyclic voltammograms shown in Figure 1 are representative of all those observed in the present study,[18] and they indicate that the monolayers fabricated here are all densely packed and contain a minority component of nearly isolated and identical redox moieties. The average formal potentials ($E^{o\prime}$) of these redox couples measured from the cyclic voltammograms are given in the fifth column

(46) Morgan, J. D.; Wolynes, P. G. *J. Phys. Chem.* **1987**, *91*, 874.
(47) (a) Marcus, R. A. *J. Chem. Phys.* **1965**, *43*, 679. (b) For simplicity, the definition of $A_{n,\mathrm{NA}}$ in eq 6 omits a factor of order unity.[17]
(48) Liu, Y.-P.; Newton, M. D. *J. Phys. Chem.* **1994**, *98*, 7162.
(49) Brunschwig, B. S.; Sutin, N. *Coord. Chem. Rev.* **1999**, *187*, 223.
(50) Sutin, N. *Prog. Inorg. Chem.* **1983**, *30*, 441.

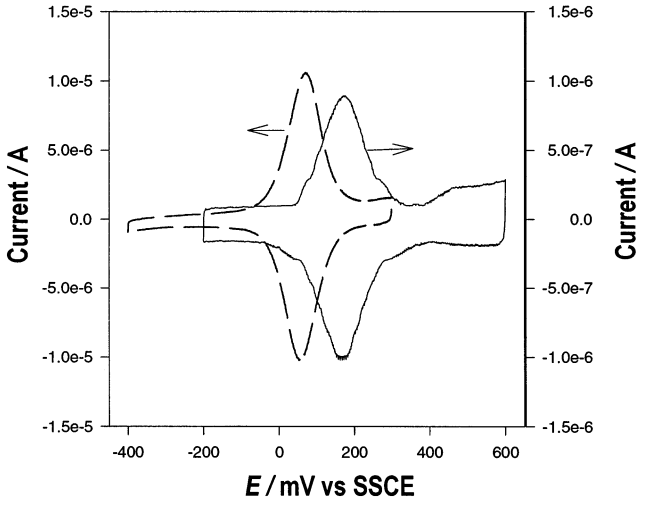

Figure 1. Cyclic voltammograms of both directly linked ferrocene (n = 11; see Table 1) and ruthenium ((pyridine)Ru(NH_3)$_5$, n = 10; see Table 1) redox couples attached to Au electrodes. Solid line (right-hand ordinate): ferrocene redox couple, $HS(CH_2)_{10}CH_3$ diluent, T = 20 °C, $FN_T = 1.08 \times 10^{-6}$ C (see eq 4). Dashed line (left-hand ordinate): ruthenium redox couple, $HS(CH_2)_{10}CO_2H$ diluent, T = 27 °C, $FN_T = 1.05 \times 10^{-5}$ C (see eq 4).

of Table 1 as a function of the length of the bridge attaching the couple to the Au electrode surface. The experimental error for all of the formal potentials reported in Table 1 is ±10 mV. The full-widths at half-maximum (fwhm) of the cyclic voltammograms are 114 ± 3 mV for the directly linked ferrocene couple and 100 ± 6 mV for the ruthenium couple. These fwhm values are a little larger than the theoretically expected value of 91 mV at 25 °C. The variation in $E^{\circ\prime}$ is slightly greater for the directly linked ferrocene redox couples than for the ruthenium redox couples, possibly indicating that the more hydrophobic (neutral) ferrocene may be interacting more strongly with the film than the hydrophilic charged ruthenium moieties. As we shall see, there is no correlation between this variation in $E^{\circ\prime}$ and the measured k° values.

Examples of the open circuit (ILIT) responses observed in this work are shown in Figure 2. Both of the ILIT transients shown in this figure are well fit by eq 2 as are all of the transients observed in the present study. At long times (for $t \gg 1/k_m$), all of the ILIT responses ($\Delta V(t)$) measured in the present study track on the interfacial temperature perturbation and approach 0 as an assymptote.[32] Furthermore, Figure 3 demonstrates that values of the experimental rate constant ($k_m(E_i)$; see eq 2) evaluated as a function of the initial potential (E_i) are well fit by eqs 3−5. Values of γ and $E^{\circ\prime}$ obtained from fits such as those shown in Figure 3 are very close (typically, within ±10% for γ and ±10 mV for $E^{\circ\prime}$) to the values obtained from the cyclic voltammograms.[35] This equivalence of the values of γ determined by cyclic voltammetry and ILIT means that both techniques are sampling the same redox populations.[35]

The sixth column of Table 1 gives the standard rate constants (k°) at 25 °C for the directly linked ferrocene and ruthenium redox couples determined from plots such as those shown in Figure 3. The measured rate constants are always well fit by the expected potential dependence (eqs 3−5), and standard rate constants reported in Table 1 are always independent of N_T (i.e., the concentration of the redox moiety in the mixed monolayer; see Figure 3). These observations confirm that the ILIT transient is, in fact, caused by an electron-transfer relaxation. The

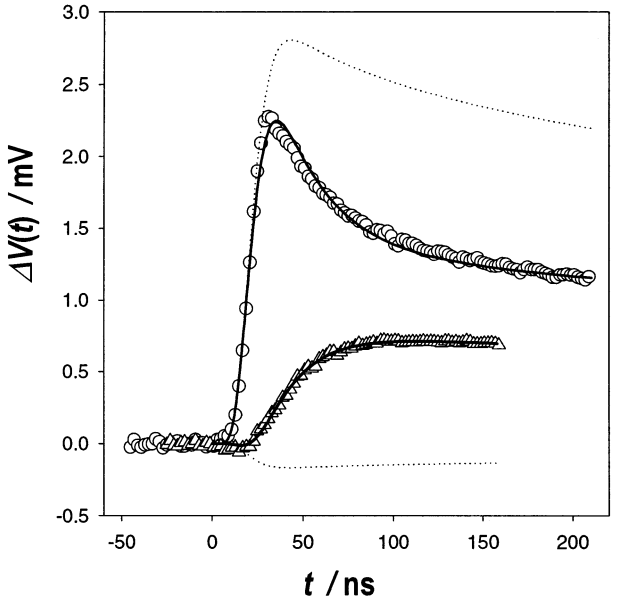

Figure 2. ILIT responses from Au electrodes coated with mixed monolayers containing either the directly linked ferrocene or the ruthenium redox moieties. ○: mixed monolayer made from $HS(CH_2)_6(\eta^5\text{-}C_5H_5)Fe(\eta^5C_5H_5)$ and $HS(CH_2)_5CH_3$ (diluent) at E_i = 150 mV vs SSCE. The solid line through these points is a fit of these data to eq 2, resulting in A' = 3.4 mV, B' = −1.6 mV, and $k_m = 3.5 \times 10^7$ s^{-1}. △: mixed monolayer made from a monolayer of dibutanoic disulfide ($[S(CH_2)_3COOH]_2$)[38] reacted with Ru(4-AMP) to give a monolayer consisting of $-S(CH_2)_3CONHCH_2$pyRu$(NH_3)_5^{3+/2+}$ and $-S(CH_2)_3COOH$ at E_i = 25 mV vs SSCE. The solid line through these points is a fit of these data to eq 2, resulting in A' = −0.21 mV, B' = +1.3 mV, and $k_m = 4.4 \times 10^7$ s^{-1}. The dotted lines represent the responses which would be observed if there were no relaxation of the ILIT signal caused by electron transfer between the electrodes and the redox couples.

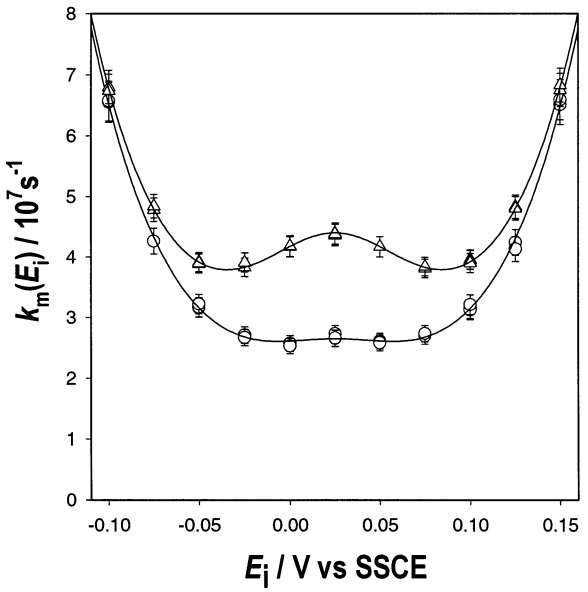

Figure 3. k_m as a function of E_i for the ruthenium ((pyridine)Ru$(NH_3)_5$) redox couple attached to Au electrodes with a bridge where n = 3 (see the caption for Figure 2). ○: the solid line through these points is the fit of these data to eqs 3 and 5, resulting in $E^{\circ\prime}$ = 25 mV vs SSCE, γ = 5.7 (see eq 4; the γ calculated from the cyclic voltammogram of this monolayer is 5.9), and $k^\circ = 5.5 \times 10^6$ s^{-1}. △: the solid line through these points is the fit of these data to eqs 3 and 5, resulting in $E^{\circ\prime}$ = 25 mV vs SSCE, γ = 12 (see eq 4; the γ calculated from the cyclic voltammogram of this monolayer is also 12), and $k^\circ = 5.4 \times 10^6$ s^{-1}.

concentration of electrolyte (0.10 or 1.0 M $HClO_4$) has no effect upon the standard rate constants (or Arrhenius activation

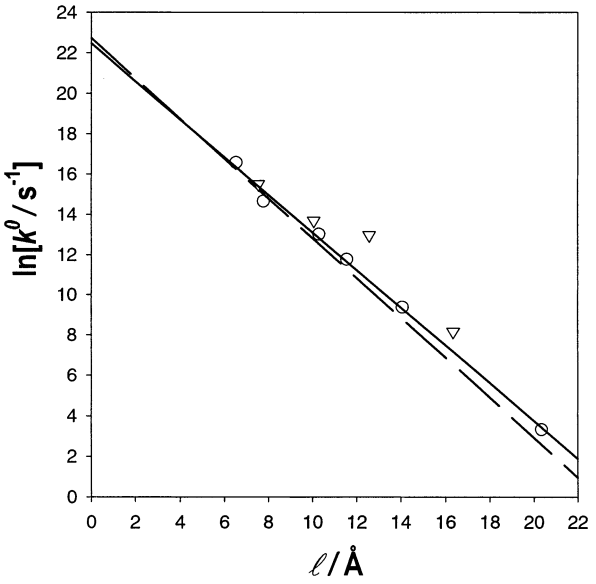

Figure 4. Natural logarithm of the standard electron-transfer rate constant ($k°$) at 25 °C for both the directly linked ferrocene (○) and the ruthenium ((pyridine)Ru(NH_3)$_3$, ▽) redox couple versus *l*. *l* is defined in footnote *c* of Table 1. The solid line describes the (least-squares) linear fit to the directly linked data (see the text). The dashed line is taken from Figure 1, ref 14, and represents the (least-squares) fit to the $HS(CH_2)_nOC(O)(\eta^5C_5H_5)Fe(\eta^5C_5H_5)$ (ester-linked ferrocene) rate constant data. The error bars for all of the data plotted in this figure are smaller than the size of the points (see Table 1).

energies or preexponential factors) measured for ferrocene. This observation verifies the claim made in the Introduction that, because the ILIT response is a change in the open circuit potential, it is unaffected by uncompensated solution resistance.

Figure 4 shows plots of ln $k°$ (determined by the ILIT technique at 25 °C) versus *l*, where *l* is the shortest distance between the carbon attached to the sulfur and the attached carbon of the redox couple to which the bridge is attached (see footnote *c* in Table 1). The parameter *l* now refers to a specific definition of the bridge length. Note that this definition of *l*, although a sensible choice, is entirely arbitrary. Also note that, for the ruthenium redox couple, *l* includes the length of the linkage. Figure 4 also contains a data point for the $k°$ (28 ± 3 s^{-1}, determined by cyclic voltammetry[18]) of directly linked ferrocene attached to the Au electrode by a bridge containing 16 methylene groups. As a comparison, the dashed line in Figure 4 is the (least-squares) linear fit to the ester-linked ferrocene $k°$ data plotted (for bridges containing 5−18 methylene groups determined by both the ILIT and chronoamperometry techniques) in Figure 1 of ref 14. (The data associated with this dashed line are not shown in Figure 4.) Note that there is very little difference between this dashed line and the solid line fitted to the directly linked ferrocene data. That is, β ($=-(\mathrm{d} \ln k°)/\mathrm{d}l$) determined from the directly linked data is 0.94 ± 0.06 Å^{-1}, while β determined from the ester-linked data is 0.99 ± 0.02 Å^{-1}. A similar equivalence (as a function of bridge length) has also been observed in a comparison[21] between the standard electron-transfer rate constants between ferrocene and gold measured (using an ac voltammetry technique[51] at $T = 25$ °C) through *n*-alkane (directly linked ferrocene) and *n*-alkylcarboxamide bridges. However, the directly linked ferrocene data plotted in Figure 4 show no clear indication of a continuation of the "even−odd effect" in the $k°$ data reported in ref 21. The ruthenium $k°$ data shown in Figure 4 are not well fitted by either the solid or dashed line in this figure.

Furthermore, for the various bridges investigated in the present study, the standard rate constants measured by ILIT are uniformly larger than those measured by ac voltammetry (for directly linked ferrocene with bridges containing either 9 or 11 methylene groups[21] or for the ruthenium redox couple with bridges containing 6, 8, or 11 methylene groups[28]). One possible explanation for these differences is that the redox monolayers investigated in the present study exhibit a heterogeneous distribution[18,26,28,52,53] of electron-transfer rate constants. However, the observation that the γ values determined by cyclic voltammetry and ILIT (eqs 3−5) are the same tends to argue against the existence of a distribution of rate constants in the monolayers investigated in the present study.

Figure 5a shows Arrhenius plots of the temperature dependence of $k°$ for both a directly linked ferrocene (whose bridge contains six methylene groups) and a ruthenium (whose bridge contains eight methylene groups) redox moiety. The seventh and eighth columns of Table 1 contain the Arrhenius activation energies (E_A, calculated as k_B times the slope of the Arrhenius plot) and the apparent reorganization energy[54] (λ_{app}, calculated using eq 7) determined from plots such as those shown in Figure 5. Figure 5b shows the Arrhenius plots determined (by chronoamperometry) for ester-linked ferrocene redox couples which were attached to Au electrodes by bridges containing 12 and 18 methylene groups. Table 2 contains the activation energies and apparent reorganization energies measured for monolayers made with these ester-linked ferrocene compounds as well as those measured (using cyclic voltammetry) for the directly linked compound whose bridge contains 16 methylene groups.

For bridges containing more than seven methylene groups, the values of reorganization energy (λ_{app}) deduced from Arrhenius analyses of the kinetic data (measured as a function of temperature) for both the ester-linked and directly linked ferrocene monolayer redox components are all the same within experimental error (see Tables 1 and 2 and Table 3 in ref 17) and the values of λ_{app} are all (also within experimental error) equivalent to the outer sphere reorganization energy of ferrocene calculated using Marcus theory (modified to take the image charge effects into account;[48] see eqs 8 and 9 and the solid and dashed lines in Figure 6). For the ruthenium couple and bridges containing 6, 8, and 11 methylene groups, all the values of λ_{app} are within the range estimated for the (essentially outer sphere) reorganization energy of the electrochemical reaction of the ruthenium hexaammine couple.[55] As has been observed previously for the ester-linked ferrocene[17] and ferrocene attached to Au electrodes by OPV bridges,[31] there is a clear (beyond experimental error; see Figure 6) decrease in E_A for the shorter bridges for both the ruthenium and directly linked ferrocene redox couples. At least for the longer bridges studied, therefore, the Arrhenius analysis performed here provides results which are consistent with theoretical expectations and previous experimental results for the (outer sphere) reorganization

(51) Creager, S. E.; Wooster, T. T. *Anal. Chem.* **1998**, *70*, 4257.

(52) Tender, G.; Carter, M. J.; Murray, R. W. *Anal. Chem.* **1994**, *66*, 3173.
(53) Napper, A. M.; Liu, H.; Waldeck, D. H. *J. Phys. Chem.* **2001**, *105*, 7699.
(54) "Apparent" because, for example, large electronic couplings can significantly lower E_A (see eq 10).
(55) Iwasita, F.; Schmickler, W.; Schultze, J. W. *Ber. Bunsen-Ges. Phys. Chem.* **1985**, *89*, 138.

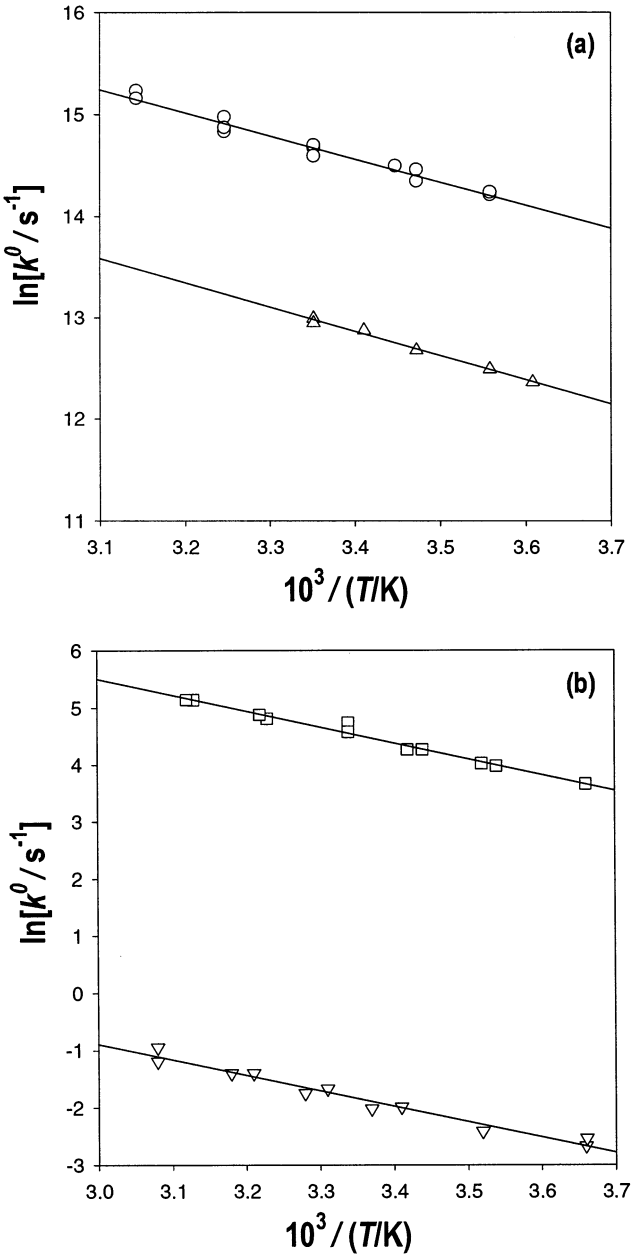

Figure 5. Arrhenius plots. (a) Semilogarithmic plots of $k°$ vs $1/T$ where the values of $k°$ are obtained from ILIT experiments on mixed monolayers containing either the directly linked ferrocene redox couple (○) attached to a Au electrode by a bridge, where $n = 6$, or the ruthenium ((pyridine)Ru(NH$_3$)$_5$) redox couple (△) attached to a Au electrode by a bridge, where $n = 7$. (b) Semilogarithmic plots of $k°$ vs $1/T$ where the values of $k°$ are obtained from chronamperometric experiments on mixed monolayers containing the ester-linked ferrocene redox couple attached to a Au electrode by a bridge, where $n = 12$ (□) or 18 (▽). The error bars for all of the data plotted in these figures are equal to or smaller than the size of the points.

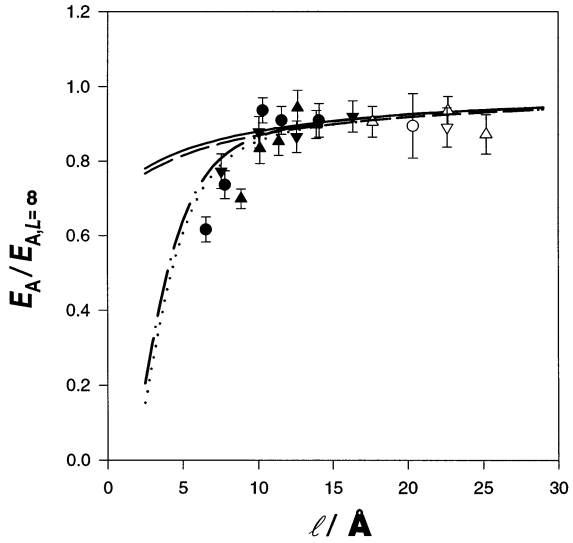

Figure 6. Ratio $E_A/E_{A,L=\infty}$ (for both the Ru and Fc redox couples, the Ru data include results taken from ref 25 and the Fc data include results taken from ref 17) versus l (see footnote *c* in Table 1), where $E_{A,L=\infty}$ is computed from eq 8 at $L = \infty$. The filled points were measured using ILIT, and the open points were measured using either chronoamperometry or cyclic voltammetry: ● and ○, directly linked Fc; △ and ▲, ester-linked Fc; ▼ and ▽, Ru couple. The solid line and dashed line are computed using eq 8 with $\epsilon_I^{op} = 1.78$, $\epsilon_{II}^{op} = 2.37$,[56] $\epsilon_I^s = 78.5$, $\epsilon_{II}^s = 2.35$,[52] $\epsilon_{III}^{op} = \epsilon_{III}^s = \infty$, a(Fc couple) = 3.40 Å,[17,45] a(Ru couple) = 3.80 Å,[57] $d = a$(for both couples), and L(both couples) = 2.1 Å + l cos(30°)[17] so that $E_{A,L=\infty} = 0.266$ and 0.238 eV for the Fc and Ru couples, respectively. The other two curves (-·- for the Fc couple and ··· for the Ru couple) are computed using both eqs 8 (for λ) and 10 for which the electronic coupling (H_{ab}) is computed using eq 13.

energies of both redox couples. This consistency also indicates that the activation entropies of both redox couples are negligibly small. However, as some of us have pointed out previously,[17] the decrease in E_A (and, consequently, λ_{app}) at short bridge lengths is too large to be explained by image charge interactions[48] (see Figure 6). This decrease in E_A (and λ_{app}) is not due to any systematic error associated with the ILIT technique; remember that the correct potential dependence (eq 3) of the measured (ILIT) rate constants is always observed (see Figure 3) and the measured standard rate constants (and, consequently, the E_A values) are always independent of the concentration of the redox moiety in the monolayer even at these short bridge lengths. (The potential dependence of $k_m(E_i)$ and concentration independence of $k°$ are very sensitive probes for systematic errors.) For the present, all we can say is that the observed decrease in E_A (and λ_{app}) is real (not due to systematic errors) but, as yet, not fully explained (see below).

The other salient parameter which is obtained from an Arrhenius analysis is the preexponential factor. These Arrhenius preexponential factors contain information on the dynamical factors (e.g., electronic coupling for a nonadiabatic reaction or, for example, the solvent longitudinal polarization rate for an adiabatic reaction limited by solvent reorganization) which affect the kinetics of electron transfer. The A_n values determined for the directly linked ferrocene and the ruthenium redox couples are plotted (versus l—defined in footnote *c* in Table 1) in Figure 7 along with the A_n values for the ester-linked ferrocene redox couple determined from both chronoamperometry and ILIT[17] experiments. (Also see the last columns in Tables 1 and 2.) As a comparison, the A_n values determined for ferrocene attached to Au electrodes by OPV bridges[31] have also been plotted in Figure 7. The first thing to note about the alkanethiol bridge data in Figure 7 is that the value determined for A_n for all these data depend solely upon l, not upon the identity of the redox couple or the functional group (linkage) to which it is attached. The reason for the equivalence (as a function of l, which includes the length of the linkage) of the $k°$ data for the directly linked and ester-linked ferrocene redox couples noted in Figure 4 is now clear. As has been proposed for the carboxamide linkage,[21] the ester linkage behaves essentially as two methylene groups. The ruthenium redox couple $k°$ values (at 25 °C; see Figure 4)

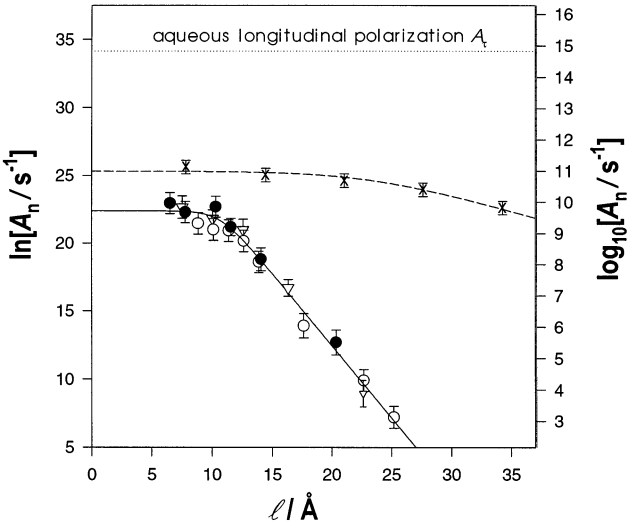

Figure 7. Semilogarithmic plots of A_n (the Arrhenius preexponential factors (see eq 1) determined in this work) for the directly linked ferrocene (●), ester-linked ferrocene (○, including data taken from ref 17), and ruthenium ((pyridine)Ru(NH$_3$)$_5$, ▽, including data at $n = 15$[25]) redox couples all attached to Au electrodes with saturated alkane bridges. The solid line is a fit of this alkane bridge data to eq 11, resulting in $I = 4.2 \times 10^{14}$ s^{-1}, $\beta_{An} = 1.06$ Å^{-1}, and $G = 8.0 \times 10^4$ and limiting at $I/(G + 1) = 5.3 \times 10^9$ s^{-1}. As a comparison, the A_n values determined for the ferrocene redox couple attached to Au electrodes with oligophenylenevinylene (OPV) bridges[31] are also plotted in this figure (×). The dashed line is a fit of these OPV data to eq 11, resulting in $I = 3.3 \times 10^{13}$ s^{-1}, $\beta_{An} = 0.25$ Å^{-1}, and $G = 3.4 \times 10^2$ and limiting at $I/(G + 1) = 0.99 \times 10^{11}$ s^{-1}. The dotted line shows the A_n expected for an interfacial electron-transfer reaction limited by solvent dynamics.[59] All of the error bars shown in this figure are at the 2σ limit.

are also somewhat different from either the ester-linked or directly linked ferrocene $k°$ values (at a corresponding value of l) simply because the activation energies of the ruthenium and ferrocene couples are somewhat different.

The most important thing to note about the alkanethiol bridge data plotted in Figure 7 is that, although, at large values of l, the logarithm of A_n is a linear function of l (as expected for A_n values determined by electronic coupling, which is, in turn, the result of a superexchange mechanism; see eq 6), A_n approaches a definite limit when l is small, and this limit is clearly different (smaller) from that observed for the ferrocene redox couple attached to Au by OPV bridges. The limiting behavior of both the alkanethiol bridge and the OPV bridge data sets are well described by the following steady-state expression:[46,58]

$$\ln[A_n] = \ln[I] - \beta_{A_n} l - \ln[1 + G \exp(-\beta_{A_n} l)] \quad (11)$$

where β_{A_n} is the exponential decay constant for A_n and the limit is determined by $I/(G + 1)$. From least-squares fits to eq 11 (the solid and dashed curves in Figure 7), the alkanethiol bridge data set limits at $A_n = 5.3 \times 10^9$ s^{-1} and the OPV data set limits at $A_n = 0.99 \times 10^{11}$ s^{-1}. (The physical significance of the parameter I is described by eq 12 below, and the physical significance of the parameter G depends on the details of the mechanism that is responsible for the turnover in the dependence of A_n upon l.) Not only are these limits approximately a factor of 19 different from each other, but they are also both orders of magnitude different from the limit that would be observed if it were due to aqueous longitudinal polarization[59] (i.e., solvent dynamics).

At large values of l, the alkanethiol bridge data set plotted in Figure 7 (for which the fitted value of I is 4.2×10^{14} s^{-1}) is well described by

$$A_n = (4.2 \times 10^{14}\ \text{s}^{-1}) \exp[-(1.06\ \text{Å}^{-1})l] \quad (12)$$

Because H_{ab} decays exponentially with distance, eq 12 describes the behavior of A_n that would be expected when the electronic coupling between the electrode and the redox moiety is determined by a superexchange mechanism (i.e., the electron-transfer reaction is nonadiabatic). If the density of electronic states in the Au is assumed to be 0.27 eV^{-1},[62] eq 6 may then be used to obtain

$$H_{ab} = (0.76\ \text{eV}) \exp[-(0.53\ \text{Å}^{-1})l] \quad (13)$$

If it is assumed that the alkanethiol bridge electronic couplings are given by eq 13 over the entire range of l investigated (even where A_n limits), eqs 8−10 and 13 may be used to calculate the alkanethiol bridge activation energies as a function of l. The results of such a calculation (see Figure 6) demonstrate reasonable agreement with the observed behavior of E_A as a function of l for both the Fc and Ru redox couples.

Equation 13 compares remarkably well with a fit (to a single-exponential decay as a function of l) of the absolute values of H_{ab} for both the directly linked and ester-linked (all-trans) alkanethiol-bridged ferrocene redox couple calculated (for $n \leq 16$) by Hsu[63] (using the sequential formula method developed by Hsu and Marcus[64]), i.e.

$$H_{ab} = (0.24\ \text{eV}) \exp[-(0.52\ \text{Å}^{-1})l] \quad (14)$$

The approximate factor of 3 difference in the preexponential factors in eqs 13 and 14 should not be considered significant considering the experimental errors involved in the determination of eq 13 and, most especially, the difficulties involved in calculating absolute values for electronic couplings.[63] At large values of l, therefore, the behavior of the alkanethiol bridge data plotted in Figure 7 is entirely consistent with a nonadiabatic (superexchange) electron-transfer process which is, surprisingly, independent of the chemical nature (pentaaminepyridine ruthenium or ferrocene) of the redox couple. (Remember that our definition of l, although reasonable, is arbitrary so that, for example, if l were extended all the way to the Fe and Ru metal centers, the A_n data might not overlap. However, the ferrocene and ruthenium redox couples' A_n values would still limit at the same magnitude of A_n.) At small values of l for both alkanethiol-tethered redox couples and both linkages of the ferrocene redox couple, the behavior of A_n is suggestive of an adiabatic electron-

(56) Billmeyer, F. W., Jr. *Textbook of Polymer Science*; John Wiley: New York, 1962; p 502.
(57) Elson, C. M.; Itzkovitch, I. J.; McKenney, J.; Page, J. S. *Can. J. Chem.* **1975**, *53*, 2922.
(58) Hynes, J. T. *J. Phys. Chem.* **1985**, *90*, 3701.
(59) The temperature dependence of the reciprocal of a solvent's longitudinal relaxation time (τ_L) may be described by $1/\tau_L = A_\tau \exp[-E_\tau/k_BT]$. For water, the data in refs 60 and 61 give $A_\tau = 6.8 \times 10^{14}$ s^{-1} and $E_\tau = 0.15$ eV.
(60) Eisenberg, D.; Kauzmann, W. *The Structure and Properties of Water*; Oxford University Press: New York, 1969.
(61) Barthel, J.; Bachhuber, K.; Buchner, R.; Hetzenauer, H. *Chem. Phys. Lett.* **1990**, *165*, 369.
(62) Royea, W. J.; Fajardo, A. M.; Lewis, N. S. *J. Phys. Chem. B* **1997**, *101*, 11152.
(63) Hsu, C.-P. *J. Electroanal. Chem.* **1997**, *438*, 27.
(64) Hsu, C.-P.; Marcus, R. A. *J. Chem. Phys.* **1997**, *106*, 584.

transfer reaction, but an adiabatic electron-transfer reaction whose rate is not controlled (limited) by solvent dynamics.

The behavior of the alkanethiol preexponential factors (A_n) at small values of l might still be indicative of an interfacial electron-transfer reaction whose rate is controlled by solvent dynamics if this reaction has a large negative activation entropy, i.e., a "tight" transition state.[31] We have already commented that the behavior of E_A (and λ_{app}) at long bridge lengths indicates that the activation entropies of both redox couples are negligibly small. Also, chemically, the ferrocene and pentaaminepyridine ruthenium redox couples are very different (e.g., the ruthenium redox moiety is a +3/+2 couple and ferrocene is a +1/0 couple). Any activation entropies for these two couples might be expected to be very different,[65] and the limits for A_n might be expected to be very different. Because this is not the case and the ferrocene/OPV bridge (A_n) limit is larger than the alkanethiol bridge limit, the rates of the interfacial electron-transfer reactions studied here and in ref 31 are not controlled by solvent dynamics.

We emphasize that the alkanethiol A_n limit shown in Figure 7 does not depend on either the identity of the redox couple or the nature of the linkage which attaches the ferrocene redox couple to the alkane chain, and that this limit is considerably different from the OPV A_n limit. A process (or processes) associated with the alkane chain constituents of the alkanethiol bridges or the OPV bridges themselves must, therefore, be responsible for these limits. There are two sets of phenomena which provide a possible explanation for the limits seen in Figure 7.

(1) The bridge-mediated electronic coupling reaches an upper bound (i.e., limits), and the electron-transfer reaction remains nonadiabatic so that A_n is determined by H_{ab}. However, a number of theoretical studies of the electronic coupling through trans-staggered (all-trans) alkane bridges[66−70] have demonstrated that the electronic coupling does not limit in the range of alkane bridge lengths investigated in the present study. Alternatively, it is known that the structural order of alkanethiol SAMs decreases with decreasing monolayer thickness,[71,72] that one aspect of this decrease in structural order is the production of gauche defects in the no longer trans-staggered alkane chains comprising the monolayer,[72] and that, in theory,[73] gauche defects decrease the electronic coupling through an alkane chain. This decrease in the structural order of the SAM as the bridge length of the alkane chain constituent of the bridge decreases might be responsible for the alkanethiol preexponential factor limit shown in Figure 7 as well as be an alternative reason (see Figure 6) for the decrease in the activation energies seen at short bridge lengths. However, because we cannot be more quantitative, this proposal must remain only a possibility. Furthermore, increased monolayer disorder in very thin alkanethiol SAMs does not provide a reason for the OPV preexponential factor limit, which is also shown in Figure 7.

(2) When A_n limits, the kinetics of the electron-transfer reaction is no longer controlled by the electronic coupling but by the dynamics of a slow (bridge) structural change accompanying the electron transfer itself.[31,74−76] These dynamics should be different for different types of bridges, which, therefore, can explain the different limiting values of A_n seen with the OPV and alkanethiol bridges. In simplest terms, an unreactive conformer of the bridge converts to a reactive conformer, and A_n is, consequently, limited by the rate of this conversion. This proposed conformational conversion is (at least formally) equivalent to a "gating" mechanism.[36−38,74−76] There may be an activation energy associated with this conformational gating of the electron-transfer reaction.[74] However, for a heterogeneous electron-transfer reaction, the electrode potential affects the activation barrier and not the preexponential factor in a simple Arrhenius model. An electron-transfer mechanism involving conformational gating is, therefore, consistent with our experimental observations in that the kinetics of the conformational reorganization process will not perturb the potential dependence of the interfacial electron-transfer kinetics.

We do not have enough information at present to determine the details of the mechanism (or mechanisms) responsible for the entire distance dependences of A_n for both the alkanethiol and OPV bridges. Nevertheless, the data obtained in the present study do suggest a number of further experiments. For example, measurements of A_n (as a function of l) in a variety of solvents (i.e., as a function of different longitudinal relaxation times) will, for example, absolutely verify that there is no relationship between the polarization dynamics of the solvent and Arrhenius preexponential limits such as those shown in Figure 7. Experiments in organic solvents may also be performed over an extended temperature range,[74,77] thereby enabling one to better elucidate the details of the electron-transfer mechanism.[74]

Conclusions

In summary, we have demonstrated for the electron-transfer reactions of the ferrocene and the pentaaminepyridine ruthenium redox couples attached to Au electrodes through alkanethiol bridges which are a part of a self-assembled monolayer that (1) the Arrhenius preexponential factors for the standard rate constants of these reactions approach a definite limit at small values of the alkanethiol bridge length, (2) this limit is (within experimental error) independent of both the identity of the redox couple (ferrocene or ruthenium) and (for ferrocene) the nature of the linkage between the redox couple and the alkane chain portion of the bridge, and (3) most importantly, this limit is different (lower) from that observed with the ferrocene redox couple attached to Au electrodes through OPV bridges and is

(65) These conclusions are consistent with the observations that the experimental λ_{app} values seen at long bridge lengths are the same (within experimental error) as the anticipated values of the outer sphere reorganization energies of the ferrocene and ruthenium redox couples, and that the activation entropies of both redox couples are negligibly small.
(66) Bragd, M.; Larson, S. *Int. J. Quantum Chem.* **1992**, *44*, 839.
(67) Curtis, S. A.; Nateway, C. A.; Miller, J. K. *J. Phys. Chem.* **1993**, *97*, 4050.
(68) (a) Paddon-Row, M. N.; Shephard, M. J.; Jordan, K. D. *J. Am. Chem. Soc.* **1993**, *115*, 3312. (b) Paddon-Row, M. N.; Shephard, M. J.; Jordan, K. D. *J. Phys. Chem.* **1993**, *97*, 1743.
(69) Liang, C.; Newton, M. D. *J. Phys. Chem.* **1993**, *97*, 3199.
(70) Kaga, N.; Sameshima, K.; Morokama, K. *J. Phys. Chem.* **1993**, *97*, 13117.
(71) For example, Nuzzo, R. G.; Korenic, E. M.; Dubois, L. H. *J. Chem. Phys.* **1990**, *93*, 767.
(72) Schreiber, F. *Prog. Surf. Sci.* **2000**, *65*, 151.
(73) (a) Newton, M. D. *Chem. Rev.* **1991**, *91*, 767. (b) Jordan, K. D.; Paddon-Row, M. N. *Chem. Rev.* **1992**, *92*, 395.
(74) Davis, W. G.; Ratner, M. A.; Wasielewski, M. R. *J. Am. Chem. Soc.* **2001**, *123*, 7877.
(75) Chi, Q.; Zhang, J.; Andersen, J. E. T.; Ulstrup, J. *J. Phys. Chem. B* **2001**, *105*, 4069.
(76) Avila, A.; Gregory, B. W.; Niki, K.; Cotton, T. M. *J. Phys. Chem. B* **2000**, *104*, 2759.
(77) Richardson, J. N.; Peck, S. R.; Curtin, L. S.; Tender, L. M.; Terill, R. H.; Carter, M. T.; Murray, R. W.; Rowe, G. K.; Creager, S. E. *J. Phys. Chem.* **1995**, *99*, 766.

orders of magnitude smaller than the limit which would be expected on the basis of the longitudinal polarization rate of water.

The effect of this limiting behavior of the Arrhenius preexponential factors on the standard rate constants at 25 °C through the alkanethiol and OPV bridges should be emphasized. For both the directly linked and ester-linked ferrocene/alkanethiol (bridge) rate constants at this temperature there is an accidental compensation[17] between the decrease in E_A and the turnover in A_n observed at short bridge lengths. The measured ferrocene (redox couple)/alkanethiol (bridge) rate constants, therefore, continue to vary exponentially with bridge length at these short bridge lengths. No such "accidental compensation" exists for the ruthenium (redox couple)/alkanethiol (bridge) rate constants at 25 °C (see Figure 4) and, because the electronic coupling through an OPV bridge is much stronger than that through an alkanethiol bridge at a particular length of the bridge,[31] for the ferrocene (redox couple)/OPV (bridge) rate constants at 25 °C (see Table 1 of ref 31).

As was mentioned in the Introduction, the rapidly increasing interest in the development of electronic devices based upon molecular materials has focused attention upon the physical and chemical parameters controlling the kinetics of electron transfer across interfaces between conventional electrodes and these materials.[31] It has also long been recognized[13] that single molecule donor−spacer−acceptor structures might very well be made to perform the basic functions of electronic circuit elements—e.g., rectification.[78] More recently,[79,80] nanometer-sized molecular structures (i.e., "bundles" of molecules[80]) have also been investigated as possible candidates for these electronic circuit elements—e.g., switches[80] and field-effect transistors.[81] Because the metallic electrode−bridge− redox couple arrangements investigated in the present study correspond to donor−spacer−acceptor structures, it would be of interest to ask whether the results reported here are relevant to the construction and understanding of the basic circuit elements needed for a molecular electronic device.[81] As an example, the bridge in these structures may be identified as a molecular scale resistor. Recognizing that, for an electrochemical electron-transfer reaction, A_n describes the rate of electron transport through the bridge,[4c] the resistance (R_{mr}) of this resistor is given by[82]

$$R_{mr} = 2k_B T/A_n e^2 \qquad (15)$$

If $A_n = 7.1 \times 10^9\ s^{-1}$ (the A_n observed for the directly linked ferrocene redox couple when $n = 8$), $R_{mr} = 4.5 \times 10^7\ \Omega$. This resistance is considerably less than that which has recently been reported[84] for the *n*-octanedithiol single-molecule nanojunction (i.e., $(9.0 \pm 0.5) \times 10^8\ \Omega$). The difference between our calculated resistance and that reported in ref 84 may well have to do with differences in the mechanism (physics) of electron transport between the two types of systems investigated.[85] It is, therefore, important to study a diversity of types of single-molecule junctions to fully understand all aspects of electron transport (such as the unexpected limits seen in the Arrhenius preexponential factors observed here and in ref 31) in these junctions.

Acknowledgment. J.F.S., K.C., S.W.F., and M.D.N. gratefully acknowledge the support of the U.S. Department of Energy, Contract No. DE-AC02-98CH10886. J.F.S. also thanks Prof. Edmond F. Bowden, Department of Chemistry, North Carolina State University, for the gift of the dibutanoic acid disulfide. M.R.L. thanks the Fannie and John Hertz Foundation for their kind support. H.O.F. thanks the National Science Foundation for support (Grant CHE-9711779). S.E.C. also thanks the National Science Foundation for support.

JA028458J

(78) Arram, A.; Ratner, M. A. *Chem. Phys. Lett.* **1974**, *29*, 277.
(79) Tour, J. M. *Acc. Chem Res.* **2000**, *33*, 791.
(80) Donhauser, Z. J.; Mantooth, B. A.; Kelly, K. F.; Bumm, L. A.; Mannell, J. D.; Stapleton, J. J.; Price, D. W., Jr.; Rawlett, A. M.; Allara, D. L.; Tour, J. M.; Weiss, P. S. *Science* **2001**, *292*, 2303 and references therein.
(81) Schön, J. H.; Meng, H.; Bao, Z. *Nature* **2001**, *413*, 713.
(82) A system consisting of a number (N_T; see eq 4) of redox moieties attached to an electrode surface as a constituent of a SAM may be viewed as $L_A N_T$ (where L_A is Avogadro's number) parallel resistors. Additionally, the activation energies of the interfacial electron-transfer reactions studied here are, to a first approximation, affected by solvent reorganization, not by any property associated with the rate of electron transport through the bridge. The (standard) rate constant for electron transport through a molecular resistor (i.e., a bridge) may, consequently, be identified as A_n.The linearized Butler−Volmer expression,[83] therefore, gives eq 15.
(83) Bard, A. J.; Faulkner, L. R. *Electrochemical Methods*; John Wiley: New York, 1980; pp 103−105.
(84) Cui, X. D.; Primak, A.; Zarate, X.; Tomfohr, J.; Sankey, O. F.; Moore, A. L.; Moore, T. A.; Gust, D.; Harris, G.; Lindsay, S. M. *Science* **2001**, *294*, 571.
(85) Nitzan, A. *J. Phys. Chem. A* **2001**, *105*, 2677.